

Optimization and control for output characteristics of He–Sr⁺(Ca⁺) recombination lasers

G.D. Chebotarev, E.L. Latush, and A.A. Fesenko

*South Federal University,
Physics Faculty, Quantum Radiophysics Department, Rostov-on-Don*

Received March 27, 2008

Experimental optimization of self-heated He–Sr⁺(Ca⁺) recombination lasers of different geometries is carried out. Regularities and tendencies in the behavior of the discharge excitation parameters and output characteristics are revealed. The physical processes determining these regularities are established. The capability of fast variation of output laser characteristics with the help of additional controlling current pulses formed in the discharge near afterglow is demonstrated. The dependences of output characteristics on characteristics of controlling pulses are calculated with the help of the mathematical modeling.

Introduction

The He–Sr⁺(Ca⁺) lasers belong to the class of metal vapor ion recombination lasers.^{1–4} They generate at 430.5 and 416.2 nm of SrII lines and at 373.7 and 370.6 nm of CaII lines. When exciting active medium by short current pulses, there occurs two-fold ionization of metal atoms due to direct and step-wise ionization by an electron shock (ES). The pump of double strontium (calcium) ions Sr⁺⁺(Ca⁺⁺) + 2e → Sr⁺(Ca⁺) + e via collisional-radiation recombination is realized after the pulse termination; the inversion is reached due to the efficient depopulation of lower laser levels at the sacrifice of the electron deexcitation into metastable and ground states of the strontium ion.

Recombination He–Sr⁺(Ca⁺) lasers have valuable properties for practical application (short wave length, relatively high energy characteristics and efficiency), therefore, physical processes in their active media and optimization of their operation modes became recently the objects of thorough researches.^{1–18} The purpose of this work is an experimental optimization of self-

heated active elements of He–Sr⁺(Ca⁺) lasers of different geometry, as well as the search for regularities in behavior of excitation parameters and output characteristics, the analysis of physical mechanisms determining these regularities, and the search for possible ways of controlling for generation characteristics.

Five self-heated elements of the He–Sr⁺ laser of different geometries and one active element of the He–Ca⁺ laser were thoroughly studied in the experiments.

The dimensions of laser tubes (the active length l , the interior diameter d , and the active volume V), typical conditions of excitation, and generation characteristics are presented in Table.

Laser tubes Nos. 1–4 and 6 have the construction presented in Fig. 1a. In the tube No. 5 (Fig. 1b), the cathaphoretic input of strontium vapor is realized, providing for a high homogeneity of the active medium. The evaporation of strontium proceeds from the broadening in the tube channel, close to anode, in the self-heated mode.

Table. The parameters of self-heated He–Sr⁺ (430.5 nm) (tubes Nos. 1–5) and He–Ca⁺ (373.7 nm) (tube No. 6) lasers (parameters in brackets are given with accounting for overlapping the tube channel with metal pieces and electrodes: efficient optical active volume V_{opt} , specific average output power P_{sp} , laser pulse specific energy E_{sp} , and the efficiency η , calculated from actual V_{opt})

tube N	l , cm	d , cm	$V(V_{opt})$, cm	f , kHz	P_{av} , mW	P_{sp} , mW/cm ³	E , μJ	E_{sp} , μJ/cm ³	P_{pk} , W	η , %	p_{He} , atm	w_{sp} , mJ/cm ³	C , pF
1 He–Sr ⁺	45	1.5	79.5 (64.4)	5	1350	17 (21)	270	3.4 (4.2)	1080	~0.08 (~0.1)	0.7	4.5	825
2 He–Sr ⁺	25	1.0	19.6 (15.9)	8	630	32 (40)	78.8	4.0 (5.0)	394	~0.08 (~0.1)	0.9	4.8	550
3 He–Sr ⁺	20	0.6	5.66 (2.83)	10	205	37 (73)	20.5	3.6 (7.3)	103	~0.06 (~0.12)	0.8	6.0	117.5
4 He–Sr ⁺	9	0.55	2.14 (1.07)	18	70	33 (65)	3.9	1.8 (3.6)	19.5	~0.04 (~0.08)	0.9	4.8	117.5
5 He–Sr ⁺	26	0.3	1.84	30	510	277	17	9.2	85	~0.06	0.8	15	117.5
6 He–Ca ⁺	26.5	0.7	10.2 (6.8)	9.5	340	33 (50)	36	3.5 (5.3)	143	~0.04 (~0.06)	0.6	9.1	550

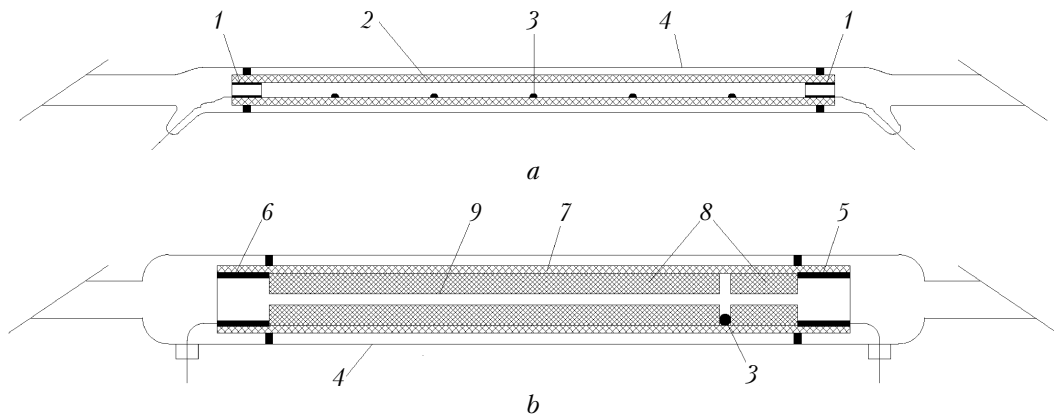


Fig. 1. Active elements of He–Sr⁺(Ca⁺) lasers: electrodes (1); a discharge tube made of BeO ceramics (2); pieces of strontium or calcium (3); exterior shell made of glass or quartz (4); anode (5); cathode (6); exterior BeO tube (7); interior BeO tube (8); active zone of the cataphoretic laser discharge (9).

Experimental oscillograms of current pulses and generation, as well as the dependences of average output power P_{av} , efficiency, specific laser pulse energy E_{sp} , pulse repetition rate f , and input power P_{in} on the helium pressure p_{He} at different values of storage capacity C for two He–Sr⁺ tubes Nos. 1 and 3 with quite different active volumes (~ 80 and ~ 5.7 cm³, respectively) are presented in Fig. 2.

As is seen, these dependences are of similar character. The same dependences were obtained for other tubes. Note that the values of specific average output power P_{sp} reached for He–Sr⁺ tube No. 3 and He–Ca⁺ tube No. 6 (73 and 50 mW/cm³, respectively, see the Table) are the maxima for self-heated He–Sr⁺ and He–Ca⁺ lasers with natural radiation and convective cooling; and value of average output power of 277 mW/cm³ is record for He–Sr⁺ lasers of all types. This value was reached in cataphoretic tube No. 5 (Fig. 1b) with intensified heat removal due to the ceramic thick wall with a great exterior surface.

As is seen from Fig. 2, P_{av} and E_{sp} maxima are reached at different p_{He} and C . Specific energy extraction $E_{sp} = 12 \mu\text{J}/\text{cm}^3$ (Fig. 2f) obtained in tube No. 3 is the maximal one achieved in longitudinal excited laser tubes at a pressure lower than 1 atm and only slightly lower than a record value of $13.8 \mu\text{J}/\text{cm}^3$, obtained at $p_{He} = 4$ atm [Ref. 12].

The increase of average generation power up to optimal pressures $p_{Heopt} \sim 0.4\div 0.9$ atm with the increase of helium pressure is observed in all tubes. At further increase of p_{He} value, exceeding the optimal one (see Figs. 2c and d), the average output power decreases. This is concerned with the increase of laser pulse generation energy (Figs. 2e and f) due to acceleration of electron cooling at elastic collisions with helium atoms and ions. Rapid cooling of electrons provides for the increase of strontium vapor pressure, and, consequently, the concentration of recombining ions Sr⁺⁺ at the maintenance of low electron temperature T_e in the early afterglowing, thus providing for the increase of rate of the pump recombination of SrII levels at p_{He} increase.

The energy input in discharge increases with the pressure augmentation, which is necessary for providing for the double ionization of the increasing number of strontium atoms. The pulse repetition rate f (Figs. 2g and h) decreases, maintaining the laser tube heat balance in the self-heated mode.

Oscillograms of current and generation pulses (Figs. 2a and b) indicate that generation pulse follows the current pulse with a short time delay, necessary for the cooling of electrons. The experiments have shown that the pressure increase up to the optimum causes the time delay decrease due to acceleration of electron cooling in afterglow.

The conducted analysis allows a conclusion that the existence of optimal helium pressure is connected with the restriction of electron cooling rate in the early afterglow due to heating impact of the current pulse trailing edge. This impact occurs when the cooling rate of electrons τ_{cool} , decreasing with the increase of p_{He} , becomes comparable with the trailing edge length of the current pulse τ_f . The length is determined by the storage capacity and the tube inductance, being almost independent of the pressure. So, at $p_{He} < p_{Heopt}$ the phase of recombination “initiation” is determined by the decay time T_e due to elastic collisions of electrons with helium atoms and ions and shortens with the p_{He} increase, while at $p_{He} > p_{Heopt}$ when the heating impact of the pulse trailing edge occurs, this phase is determined by the trailing edge length and does not depend on p_{He} .

At pressures, exceeding optimal, the share of uselessly recombining Sr⁺⁺ ions in the initial phase of recombination pump increases. This useless loss of ions takes place both before the occurrence of the lasing threshold and in the initial stage of lasing pulse, when optimal conditions for the recombination pump are not yet reached. As a consequence, the increase of the pumping rate and, consequently, pulse energy is retarded with p_{He} augmentation (Figs. 2e and f), which causes the laser efficiency decrease (Figs. 2c and d).

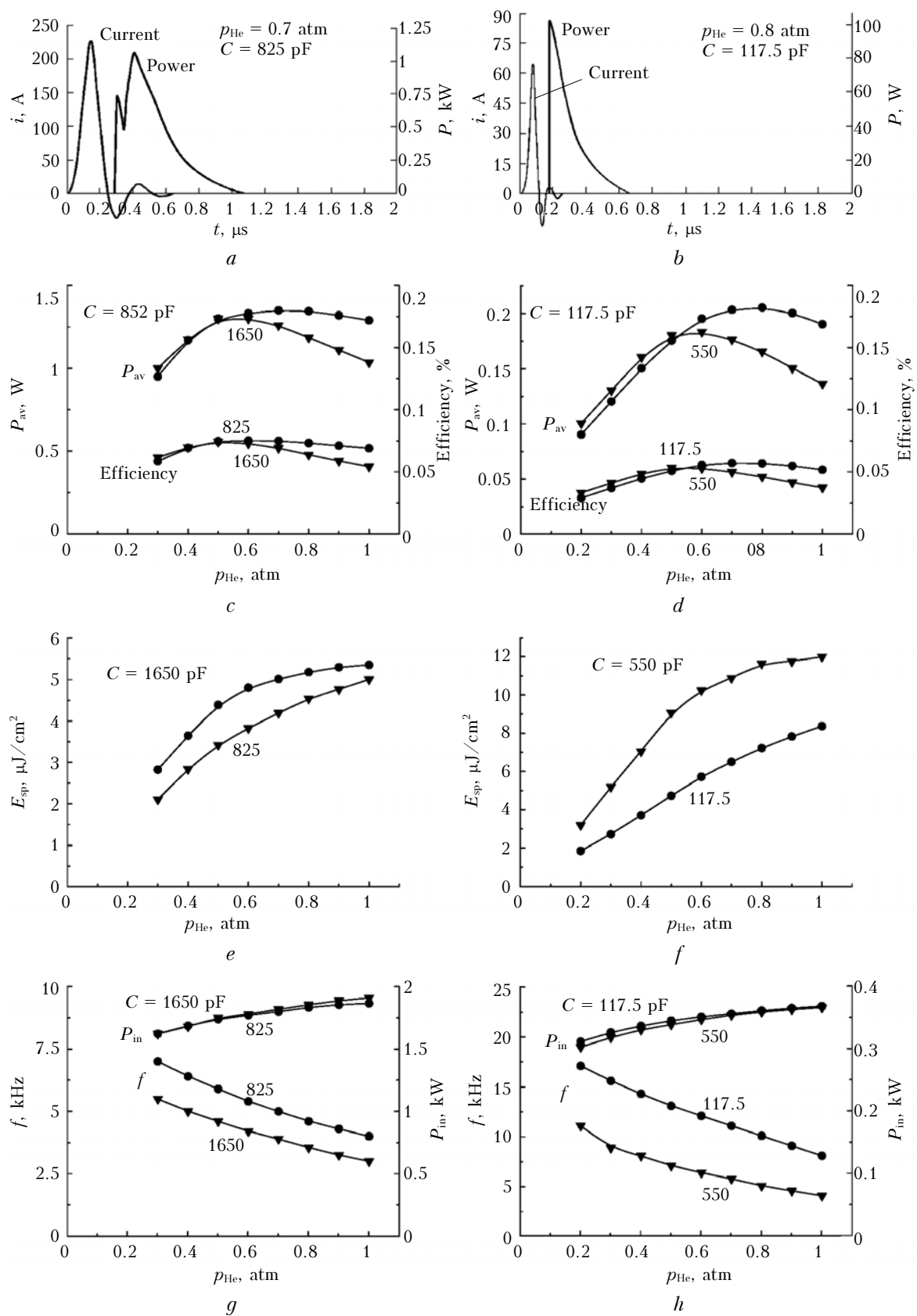


Fig. 2. Current and laser pulse oscillograms at $\lambda = 430.5$ nm SrII (a, b), as well as the dependences of helium pressure, average output power and efficiency (c, d), specific laser pulses energy (e, f), pulse repetition rate and input power (g, h) for laser tubes No. 1 (a, c, e, h) and 3 (b, d, f, h).

The average oscillation power P_{av} in self-heated mode is determined by the efficiency coefficient η and the input power from the power source P_{in} , equal to heat power Q , which is dispersed by the laser tube due to convection and heat radiation at optimal temperature of the wall: $P_{av} = \eta P_{in} = \eta Q$. The necessary increase of strontium vapor pressure with the increase of p_{He} , caused by a strong dependence of saturated vapor pressure on the wall temperature, is provided for only by a slight increase of laser tube temperature and, consequently, by a slight increase of the consumed power (see Figs. 2*g* and *h*). Due to a low dependence of laser pulse input power P_{in} on the helium pressure, the dependences of the efficiency and average input power P_{av} on the pressure almost coincide (Figs. 2*c* and *d*). Thus, a significant decrease of the efficiency at high pressures leads to the decrease of the average lasing power.

The found mechanism of limitation of the increase of recombination laser energy characteristics allows us to explain the observed experimentally augmentation of the optimal pressure $p_{He,opt}$ at decreasing storage capacity C (Figs. 2*c* and *d*). The optimal pressure does correspond to conditions of an approximate equality of electron cooling time $\tau_{cool} \propto 1/p_{He}$ and the trailing edge length of the current pulse $\tau_f \propto (LC)^{0.5}$ (L is the tube inductance summed with the inductance of the exterior chain).¹⁸ Therefore, $p_{He,opt} \propto 1/(LC)^{0.5}$. However, the possibility of varying C is limited by the necessity to satisfy the conditions of laser tube matching with the pumping scheme.

As is seen from Figs. 2*a* and *b*, at optimal regimes of the laser tube excitation, the regime of discharge circuit, formed by storage capacity C , induction L , and tube active resistance R , becomes close to the critical, which corresponds to the discharge conversion from aperiodic mode to the oscillation one. The condition of critical mode for discharge circuit $R = 2\sqrt{L/C}$ corresponds to the condition of matching tubes to the pumping scheme and is connected with the necessity to obtain maximally steep trailing edge with minimal undershoots.

The current pulse length is determined by the storage capacity and inductance; it increases with the increase of the capacity (Figs. 2*a* and *b*). Lasing pulse length is determined by the helium pressure and decreases with its increase (Figs. 2*a* and *b*). Due to the augmentation of electron concentration at maintenance of low electron temperature in early afterglow and corresponding shortening of the recombination time.

As Fig. 2*a* shows, a slight mismatching leads to the increase of extraneous pulsations in early afterglow, which, in its turn, leads to the heating of electrons and, consequently, to a dip in lasing pulses due to a strong dependence of the triple electronic recombination coefficient α on the electron temperature ($\alpha \propto T_e^{-9/2}$).¹⁻⁴ At a small storage capacity, the influence of the current pulses on the

generation pulse is minimal, because they practically cease to its beginning owing to a short current pulse length (Fig. 2*b*).

The experiments have shown that at optimal pressures the average output power maximum is gained, as a rule, not at maximal values of pulse energy output, because it corresponds to maximal efficiency, but not to the pulse energy. The existence of quite a wide range of possible variations of specific input energy in w_{sp} discharge and specific output energy E_{sp} (Table, Fig. 2), at which average power, close to maximal, can be gained, is of particular interest. Thus, a relatively high efficiency can be achieved at relatively low w_{sp} .

The experiments also have shown that in the used range of optimal pressures the specific input energy usually takes values from the range $w_{sp} \sim 2-10$ mJ/cm³. (The value of w_{sp} for cataphoretic tube No. 5 (see Table) is beyond this range as it contains the energy input into the tube part between the anode and the vaporizer, enclosing metal vapors (Fig. 1*b*)). At fixed p_{He} , the specific input energy, providing for almost maximal P_{av} , can vary by almost two times (see experimental points in Figs. 3*a* and *b*).

Taking into account the fact that optimal concentration of metal vapor is determined solely by the helium pressure (as Figs. 2*g* and *h* shows, at a fixed pressure and variable C and other excitation parameters, the consumed power and, consequently, tube temperature and strontium vapor concentration do not change), the existence of a range of w_{sp} possible values indicates that at optimal p_{He} the efficiency close to optimal can be achieved in quite a wide range of degrees of double ionization of strontium (calcium) atoms. The optimal input energy for each laser tube provides for both quite a high percentage of double ionization of metal atoms and the tube matching to the pump scheme by achieving the necessary plasma resistance. Apparently, maximal input energy depends on the tube geometry (determining its resistance at the achievable plasma conductivity) and the storage capacity (determining the matching condition). Therefore, the w_{sp} magnitude in the above range can be found by the proper selection of the capacity. Excitation modes close to optimal can be realized at variation of C values by $\sim 2-5$ times (Fig. 2). The average output power close to maximal can be obtained (Fig. 2 and Table) only at maximal (in this range) values of C , when the maximal specific input and output energy are achieved (since the matching is provided for only at minimal R and maximal plasma conductivity). It is seen from the Table, that the excitation mode for the tube No. 5 was realized at high values of P_{sp} and E_{sp} .

The lower boundary of w_{sp} possible variations corresponds to the input power, which provides for quite a high percentage of double ionization of metal atoms, necessary for a significant excess of the threshold rate of recombination pumping of the upper laser level at a concentration of electrons n_e , sufficient for efficient collisional depopulation of the

lower laser level. The upper boundary corresponds to the w_{sp} , at which practically total double ionization of strontium (calcium) occurs. When exceeding this

magnitude, the energy excess is spent to the helium ionization, thus decreasing η and P_{av} and, however, still remaining E at a high level.

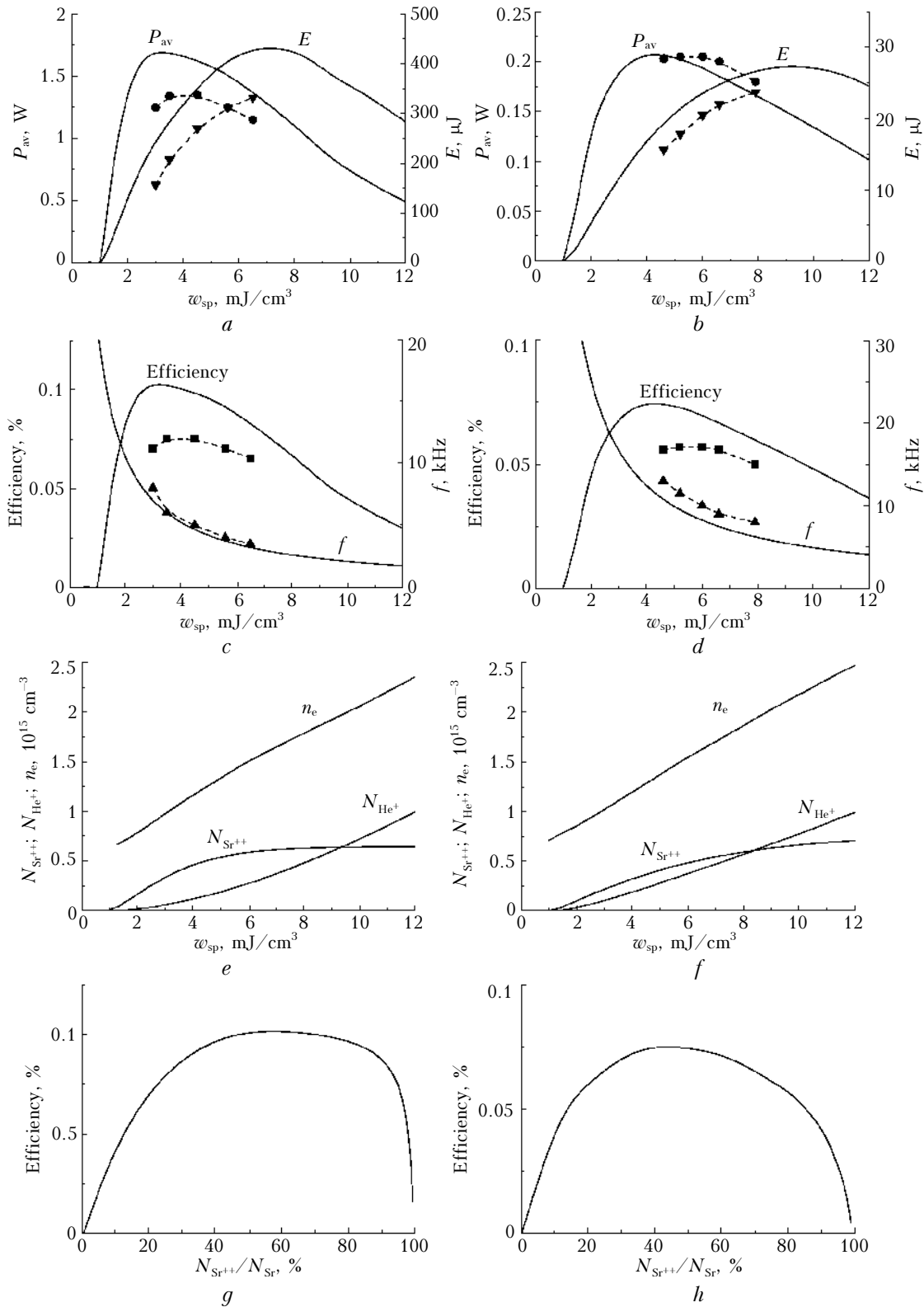


Fig. 3. The modeling results of He-Sr⁺ laser tubes No. 1 (a, c, e, g) and 3 (b, d, f, h); dots refer to experimental data: $p_{He} = 0.7$ atm, $C = 825$ pF (tube No. 1); $p_{He} = 0.8$ atm, $C = 117.5$ pF (tube No. 3)

Let us analyze the experimental results, obtained with the help of the He–Sr⁺ laser mathematical model¹⁹ for tubes Nos. 1 and 3 (see Table), presented in Fig. 3.

The dependences of P_{av} and E on w_{sp} , calculated and measured at optimal p_{He} and obtained by variations of the initial voltage of the storage capacity at invariable optimal tube temperatures, as well as strontium atom concentrations, maintained at the expense of the corresponding variations of the frequency f are shown in Figs. 3*c* and *d*. It is seen that the maximal average power is achieved at a lower input energy than the maximum of the pulse energy and coincides in practice with the efficiency maximum (Fig. 3*c* and *d*). There is quite a wide range of w_{sp} values, at which P_{av} is close to its maximum.

The growth of E is caused by the concentration increase of Sr⁺⁺ ions (Figs. 3*e* and *f*) and the corresponding increase of the recombination pump rate. The fall of E , which occurs after reaching the maximum, is due to mismatching caused by the increase of the electron concentration n_e (Figs. 3*e* and *f*) and the decrease of the corresponding plasma conductivity. The fall in efficiency and average power after reaching maximum is caused by augmentation of the energy share consumed for helium ionization. Concentrations of He⁺ and Sr⁺⁺ ions are compared at $w_{sp} \sim 8\text{--}10 \text{ mJ/cm}^3$ (Fig. 3*e* and *f*). The calculated dependence of the efficiency on the degree of double ionization of strontium atoms is shown in Figs. 3*g* and *h*. This dependence indicates that there is quite a wide range of values of the double ionization degree (~30–80%), at which sufficiently high values of the efficiency are achieved. This fact agrees with the experiment.

Let us analyze the possibility of fast control for the He–Sr⁺(Ca⁺) laser generation characteristics. The task of the fast control is particularly important for self-heated lasers, which require the stability of laser tube temperature for maintenance of optimal metal vapor pressure. This requirement excludes a possibility of controlling the generation characteristics in a wide range via variation of pulse energy input in discharge or the frequency of the excitation pulse repetition. These variations are possible only in a narrow range, that together with thermal inertia of the laser tube sharply worsens the control for generation characteristics.

Using a copper vapor laser as the example, the possibility of controlling for generation characteristics via impact the active medium by an additional controlling current pulse was shown.^{20–22} This method can also be applied to He–Sr⁺(Ca⁺) lasers, taking into account the difference in lasing mechanisms of copper vapor lasers and recombination lasers. Evidently, the control for recombination laser characteristics can be realized through imposing of a small additional current pulse on the close afterglow, heating the electrons and thus decreasing the recombination pump rate and the inversion, as well as generation energy characteristics. The control for lasing characteristics in a wide range can be realized by varying the amplitude,

length, and the moment of application the additional pulse. At a small amplitude of the controlling pulse, the total power, input in the discharge, changes insignificantly. This will allow the maintenance of stable heat mode of the laser tube and a high control efficiency.

The effect of additional short current pulses has already been investigated in Refs. 1–3, where deep valleys both in pulses of spontaneous radiation and in pulses of generation at 430.5 nm of SrII line coinciding in time with additional current pulses were described. This was a direct evidence of strong dependence of pump rate on the electron temperature, which is inherent to the recombination mechanism.

We have conducted numerical investigations of a possibility of controlling for He–Sr⁺ laser generation characteristics. The formation of controlling current pulses while modeling was actualized by application of rectangular voltage pulses with varying amplitude $U_{control}$ and the application moment t' to the gas-discharge gap.

The analysis of calculation results has shown that the decay and break of inversion under the influence of the additional controlling pulses are caused by the decrease of recombination rate of pumping the upper laser level, electron deexcitation rate of the lower laser level, as well as the increase of the rate of populating the latter from the Sr ion ground and metastable states under the electron shock impact.

The results of modeling the control for laser tube No. 1 by time variation of the additional pulse impact are shown in Fig. 4*e*, where the amplitude of $U_{control}$ and the controlling pulse length are fixed at 1.5 kV and 1 μs , respectively. Figure 4*a* illustrates the influence of such controlling pulse at the moment of its application $t' = 0.5 \mu\text{s}$, which leads to the generation pulse break. As is seen in Fig. 4*c*, illustrating temporal behavior of the temperature and electron concentration, T_e increases under the impact of the additional pulse; and fall of n_e slows down, because the recombination process is decelerated.

The impact of controlling current pulses leads to a decrease of average P_{av} and peak P_{pk} generation power (Fig. 4*f*). In this case, the laser radiation characteristics are regulated in a wide range and the curves are close to linear. Laser pulse length τ can also be well controlled. In this mode the energy input and pulse repetition rate f are stable.

The results of the modeling of the control through variation of the additional pulse amplitude are illustrated in Fig. 4*f*. In this mode, the controlling pulse of 1 μm length immediately follows the main pulse ($t' = 0.2 \mu\text{m}$). The influence of such controlling pulse at $U_{control} = 0.7 \text{ kV}$ leads to a decrease in the generation pulse amplitude without distorting its form (Figs. 4*b* and *d*).

Figure 4*f* demonstrates the adjustment of laser characteristics in a wide range. However, controlling curves are nonlinear in this mode. The generation pulse length is approximately constant, but a slight

adjustment of the frequency f is necessary because of variability of the energy input.

Thus, the obtained results allow a purposeful selection of optimal conditions and excitation parameters for recombination lasers, as well as the prediction and interpretation of the experimental

results. The possibility of fast control for output characteristics in a wide range with the help of additional controlling current pulses formed in the close afterglow is shown. The dependence of generation characteristics on parameters of the controlling pulses has been calculated.

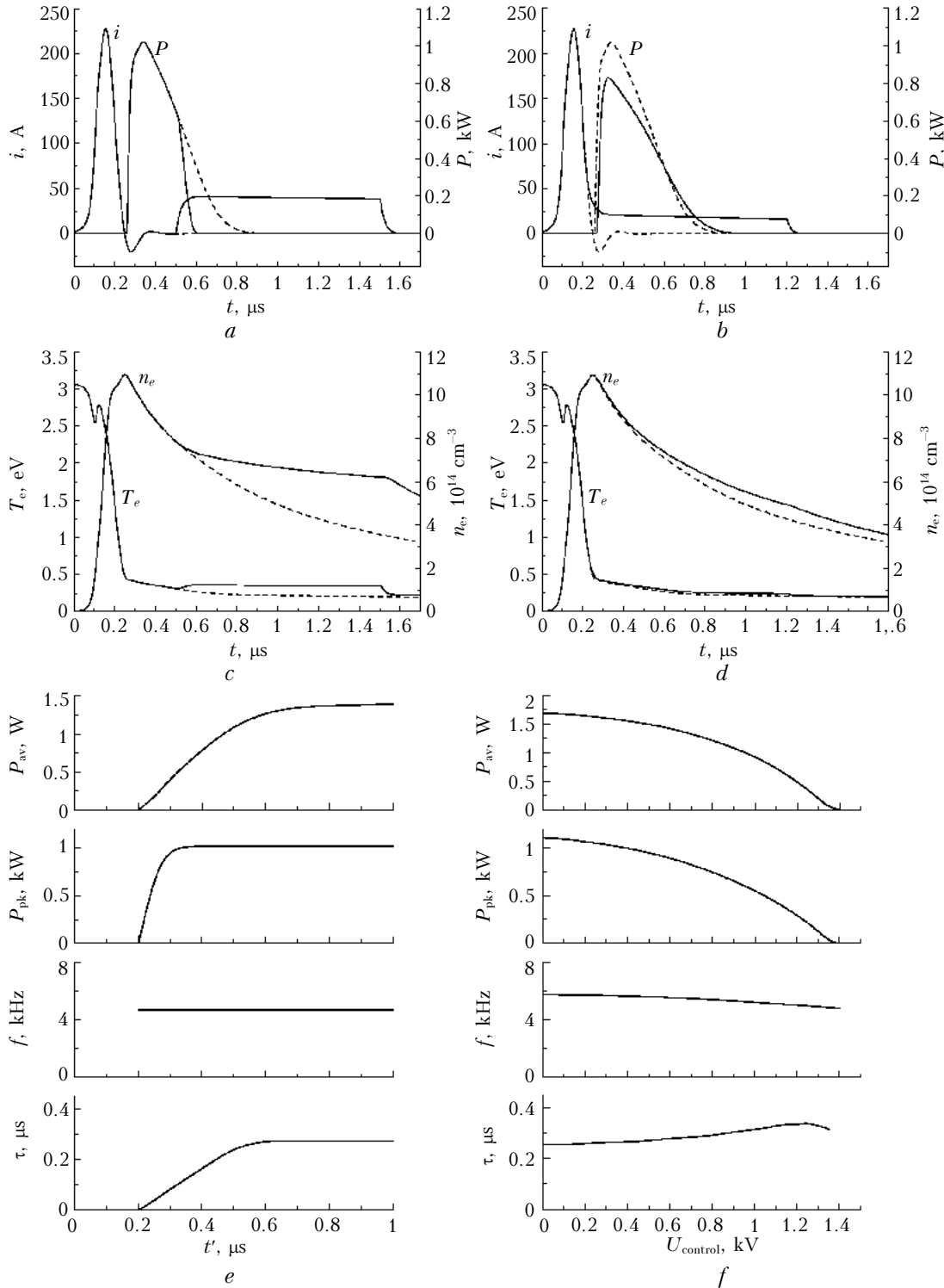


Fig. 4. The results of modeling of control for He–Sr⁺ laser characteristics (laser tube No. 1) via variation of the moment of the additional 1 μm pulse application at $U_{\text{control}} = 1.5$ kV (a, c, e) and the amplitude of the pulse at $t' = 0.2$ μm (b, d, f); dot line is a standard generation mode: $p_{\text{He}} = 0.7$ atm, $C = 825$ pF.

References

1. I.G. Ivanov, E.L. Latush, and M.F. Sem, *Metal Vapor Ion Lasers* (Energoatomizdat, Moscow, 1990), 256 pp.
2. I.G. Ivanov, E.L. Latush, and M.F. Sem, *Metal Vapour Ion Lasers: Kinetic Processes and Gas Discharges* (John Wiley & Sons, Chichester, New York, 1996), 285 pp.
3. C.E. Little, *Metal Vapour Lasers: Physics, Engineering and Applications* (John Wiley & Sons, Chichester, New York, 1999), 619 pp.
4. *Encyclopedia of Low-temperature Plasma. Gas and Plasma Lasers* (Moscow, PHYSMATHLIT, 2005), Vol. XI-4, 822 pp.
5. V.V. Zhukov, V.S. Kucherov, E.L. Latush, and M.F. Sem, *Sov. J. Quant. Electron.* **7**, No. 6, 708–714 (1977).
6. S.M. Babenko and S.I. Yakovlenko, "Process kinetics analysis in He–Sr laser," Preprint No. 3192 (1979), 40 pp.
7. V.M. Klimkin, V.E. Prokop'ev, and L.V. Fadin, *Sov. J. Quant. Electron.* **9**, No. 3, 357–360 (1979).
8. E.L. Latush, M.F. Sem, L.M. Bakshpun, Yu.V. Koptev, and S.N. Atamas', *Opt. Spectrosc.* **72**, No. 5, 1215–1228 (1992).
9. M.S. Batler and J.A. Piper, *Appl. Phys. Lett.* **45**, No. 7, 707–709 (1984).
10. M.S. Batler and J.A. Piper, *IEEE J. Quant. Electron.* **21**, No. 10, 1563–1566 (1985).
11. C.W. McLucas and A.J. McIntosh, *J. Phys. D* **20**, No. 5, 591–596 (1987).
12. S.N. Atamas', E.L. Latush, and M.F. Sem, *J. Russian Laser Res.* **15**, No. 1, 66–68 (1994).
13. N.K. Vuchkov and D.N. Astadjov, *Opt. Laser Technol.* **27**, No. 6, 407–408 (1995).
14. C.E. Little and J.A. Piper, *IEEE J. Quant. Electron.* **26**, No. 5, 903–910 (1990).
15. D.G. Loveland, D.A. Ochar, A.F. Zerouk, and C.E. Webb, *Meas. Sci. and Technol.* **2**, No. 11, 1083–1087 (1991).
16. P.A. Bokhan and D.E. Zakrevskii, *Sov. J. Quant. Electron.* **21**, No. 8, 838–839 (1991).
17. E.L. Latush, G.D. Chebotarev, and M.F. Sem, *Quant. Electron.* **30**, No. 6, 471–478 (2000).
18. G.D. Chebotarev and E.L. Latush, *Quant. Electron.* **30**, No. 5, 393–398 (2000).
19. G.D. Chebotarev, O.O. Prutsakov, and E.L. Latush, *Proc. SPIE* **5483**, 83–103 (2004).
20. A.N. Soldatov and F.V. Fedorov, *Sov. J. Quant. Electron.* **13**, No. 5, 612–615 (1983).
21. A.N. Soldatov and V.I. Solomonov, *Self-heated Transfers Gas Lasers* (Novosibirsk, Nauka, 1985), 151 pp.
22. G.S. Evtushenko, A.E. Kirilov, V.L. Kruglyakov, Yu.P. Polunin, A.N. Soldatov, and N.A. Filonova, *Zh. Prikl. Spektrosk.* **49**, No. 5, 745–751 (1988).